STM JOURNALS

International Journal of
Biochemistry and Biomolecule Research

Volume 1, Issue 1, 2023
January–June
DOI (Journal): 10.37591/IJBBR

https://journals.stmjournals.com/ijbbr/

Research IJMBR

Investigate an Implementation Study of TI-6AL-4V Lattice-based Scaffold Design Using Finite Element Analysis

Amit Bhumarker[1,*], Abhishek Singh[2]

Abstract

Implementation studies are advised to determine the effectiveness and performance of bone scaffolding in morphology, which has been demonstrated scientifically. The rehabilitation of bone defects, which is still a complex problem in orthopedic surgery, was the subject of an implementation study we provided. Biomaterial scaffolding porosity and pore size are essential in both in vivo and in vitro bone development. However, it has been linked to various drawbacks, including poor effective damping, low amounts of deformation, poor capability for absorbing energy, and mismatched bone strength and Young's modulus (E). Therefore, metallic materials like titanium and its alloy have been studied to treat bone deformities. The research studied the mechanical characteristics of four distinct unit-cell-based architectural scaffolds. Biomaterial scaffolds with predetermined pore size and porosity were created using IntraLattice and Blender 3D software. To determine the Johnson-Cook model's effectiveness in predicting the mechanical behavior of scaffold structures, quasi-static finite element (FE) analysis simulations using commercial CAE software were conducted. Similar to human cortical bone, the mechanical characteristics of yield strength (YS) and ultimate Young's modulus (E) were examined. Between 2.59 and 7.65 GPa was determined to be the elastic modulus based on finite element studies.

Keywords: Porosity, pore size, unit cell, finite element analysis, scaffold

INTRODUCTION

Currently, a variety of biomaterials, including bio-ceramics, biopolymers, bio-composites, and bio-metals, are accessible. These materials are crucial for joint replacement and the development of bone tissues [1]. In contrast to bones, however, the high modulus of dense biomaterials makes stress-shielding difficult. Therefore, bone resorption is the primary issue with dense metallic materials in orthopedic surgery [2]. Compared to dense and coated biomaterials, porous structures illustrate the intrinsic necessity for bone in-growth based on porous design characteristics such as strut diameter, length, pore size, and porosity. Although porous ceramics and polymeric biomaterials have been examined as intrinsic bone graft replacements [3], they cannot fulfill the required specifications of load-bearing applications [4]. Accordingly, porous bio-metals such as titanium, titanium-nickel, and tantalum have been studied. Ti6Al4V has excellent corrosion resistance, a high strength-to-weight ratio, biofunctionality, biocompatibility, and bio-adhesion (bone growth). The primary issue with

*__Author for Correspondence__
Amit Bhumarker
E-mail: amitbhumarker2@gmail.com

[1]Assistant Professor, Department of Mechanical Engineering, Annie Institute of Technology and Research Centre, Chhindwara, Madhya Pradesh, India
[2]Assistant Professor, Department of Mechanical Engineering, Annie Institute of Technology and Research Centre, Chhindwara, Madhya Pradesh, India

Received Date: April 03, 2023
Accepted Date: May 01, 2023
Published Date: May 15, 2023

Citation: Amit Bhumarker, Abhishek Singh. Investigate an Implementation Study of TI-6AL-4V Lattice-based Scaffold Design Using Finite Element Analysis. International Journal of Biochemistry and Biomolecule Research. 2023; 1(1): 28–35p.

metallic implants in orthopedic surgery is the mechanical mismatch between bone and implant materials. This mechanical divergence prevents the bone from being adequately loaded and causes it to become stress-shielded, which inevitably causes bone resorption [5]. Cellular structures have the benefits of being lightweight, effective damping, high-grade deformation, superior energy absorption capabilities, durable under dynamic loadings, and fatigue-resistant [6].

BACKGROUND OF LATTICE-BASED CELLULAR STRUCTURE BIOMATERIAL

Many biomaterials are currently accessible, including bio-ceramics, biopolymers, bio-composites, and bio-metals. These materials are crucial for joint replacement and the in-growth of bone tissues [7]. However, because of their higher modulus than bones, dense biomaterials present the issue of stress-shielding. Bone resorption is the primary issue with dense metallic biomaterials used in orthopedic surgery [2]. The porous structures show inherent bone in-growth, which would depend on porous design factors such as strut diameter, strut length, pore size, and porosity, as opposed to dense and coated biomaterials.

In contrast, porous ceramics and polymers have been investigated as natural alternatives to bone grafts [8]. However, they cannot satisfy the mechanical needs of applications requiring load-bearing [9]. As a result, research has been done on porous bio-metals such as tantalum, titanium, and titanium-nickel. Ti-6Al-4V possesses excellent biocompatibility, biofunctionality, bio-adhesion (bone formation), and corrosion resistance [10]. Metal additive manufacturing (AM) processes like selective laser melting (SLM) and electron beam melting (EBM) are used to create intricate metallic micro-lattices [11]. Unlike traditional production methods, additive manufacturing may create Ti-6Al-4V cellular structures with the same mechanical characteristics as genuine bone. Due to their lightweight and sturdy construction, MLS provides intrinsic benefits over foams [12]. In orthopedic surgery, designing the desired porosity of Ti-6Al-4V porous scaffolds is necessary to repair injured hard tissues (bone) [13].

Using 3D printing, bone scaffolds are created to replace damaged tissue with biodegradable material with the necessary mechanical characteristics. Most 3D printer inks that make bone or cartilage are naturally stiff [14]. Osteointegration is the term used to describe the direct structural and functional relationship between bone and implant. When an implant is put into the bone, bone-implant contact is formed between the implanted biomaterial's surface and the surrounding bone. To summarize the findings of a critical review performed on poly-ether-ether-ketone (PEEK) and its composite materials for medical applications, such as cellular calcium hydroxyapatite (cHAp) [15]. The pores of bone tissue, which play a crucial role in bone regeneration, could mimic the areas of nanoparticles on porous scaffolds. It is developed and manufactured as a one-of-a-kind nanostructured surface of polyetheretherketone-reduced graphene oxide and calcium hydroxyapatite (PEEK-rGO-cHAp) composite scaffolds with diverse lattice architectures [16].

Calcium hydroxyapatite (cHAp) composites are created in three dimensions (3D) on scaffolds made of PEEK and similar materials. A composite material with superior mechanical, thermal, and flow characteristics for biocompatibility and bone implants, the combination is constructed of coated biocompatible PEEK and cHAp. The PEEK/cHAp interface interactions that facilitate biological fusion are studied for novel biomedical applications. This study examines traditional coating methods for cHAp and PEEK fusion interfaces and in vitro and in vivo analyses of the interactions between proteins and composites to demonstrate biocompatibility [17].

Materials for artificial bone implants must have porosity to distribute nutrients, moderate pore size to support cell cultures, and mechanical qualities similar to those of bone. An essential factor is the homogenization of differences in the microstructure of implants and bone. Using PEEK and its composites to develop microstructures to enhance implant compatibility. The PEEK and hip implant composites-controlled homogenization, porosity, and particle size distribution promote cellular

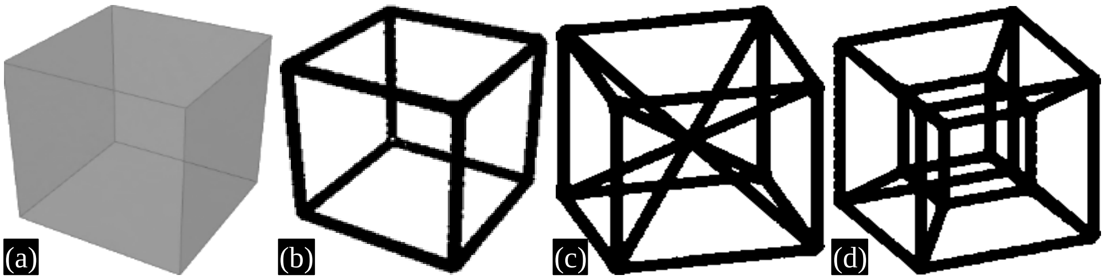

Figure 1. Unit cell topologies. (a) Unit shape volume, (b) grid, (c) star, and (d) tesseract.

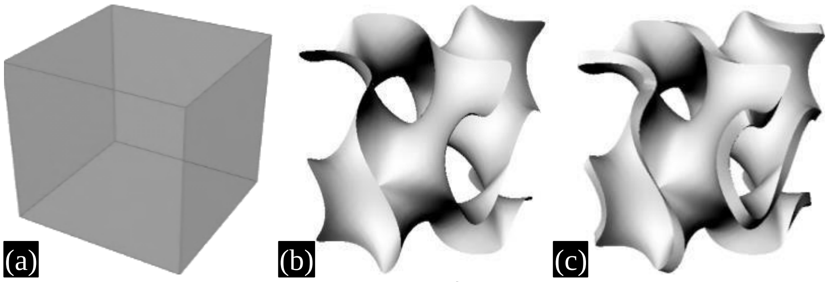

Figure 2. Triply periodic minimal surface. (a) Unit shape volume, (b) Gyroid 3D surface, (c) Gyroid 3D solid.

penetration and biological integration [18]. Poly-ether-ketone (PEEK) is a bioactive material that could replace metal and ceramic parts in biomedical applications. However, it lacks some of the real bone's strength and biological properties. To increase the interface's biocompatibility and make it more resemble bone, calcium hydroxyapatite (cHAp) and reduced graphene oxide (rGO) were mixed with PEEK and various lattice porous patterns were created [19]. Examine the existing issues with printing PEEK and cHAp and the potential applications for these materials. Based on scientific processes, prospective modifications to enhance the 3D printability of PEEK and cHAp are presented [20]. The most significant disadvantage of PEEK implants is their biologically inert surface, which leads to inadequate cellular response and poor adhesion between the implants and surrounding soft tissues, hence inhibiting healthy bone development [21].

The mechanical performance of cHAp-coated PEEK is better because the degree of crystallinity has increased, and residual polymer has built up [22]. The computational characterization of the nanostructure and finite element analysis (FEA) of PEEK/hydroxyapatite (HAP) and graphene oxide (GO) to solve the problems of high melting temperature and poor adhesion and make it possible to achieve the lightweight characteristic [23]. This part of the research is caused by the fact that various micro-lattice model types with the same pore size and diameter can change the mechanical response to the same loading scenario. Instead of using a unit shape volume definition, four distinct unit cell topologies—grid (G), star (S), tesseract (T), and gyroid are described in this study (Figures 1 and 2). Star and tesseract have a similar outer wireframe to grid but have different internal architectures. The software IntraLattice, created by McGill's Additive Design and Manufacturing Laboratory (ADML, 2016), was used to generate the MLS. It is based on the grasshopper graphic algorithm editor for Rhino CAD software. Similarly, the thickness and height of the gyroid unit shape model's struts are the same as those of the unit lattice structure. The gyroid form was created using Blender CAD software.

METHOD SIMPLIFICATION

Modeling Approach and Simplification

The model of the micro-lattice structure had dimensions of 2 mm in height, 1.5 mm in pore size, and 0.5 mm in strut diameter. A gyroid unit shape model has a height of 2 mm and a thickness of 0.5 mm, corresponding to the studied lattice's height and strut diameter. In Figure 3, unit cells of a 5×5×5 array are shown. Table 1 shows the geometric properties of the four-unit cell (lattice) structure.

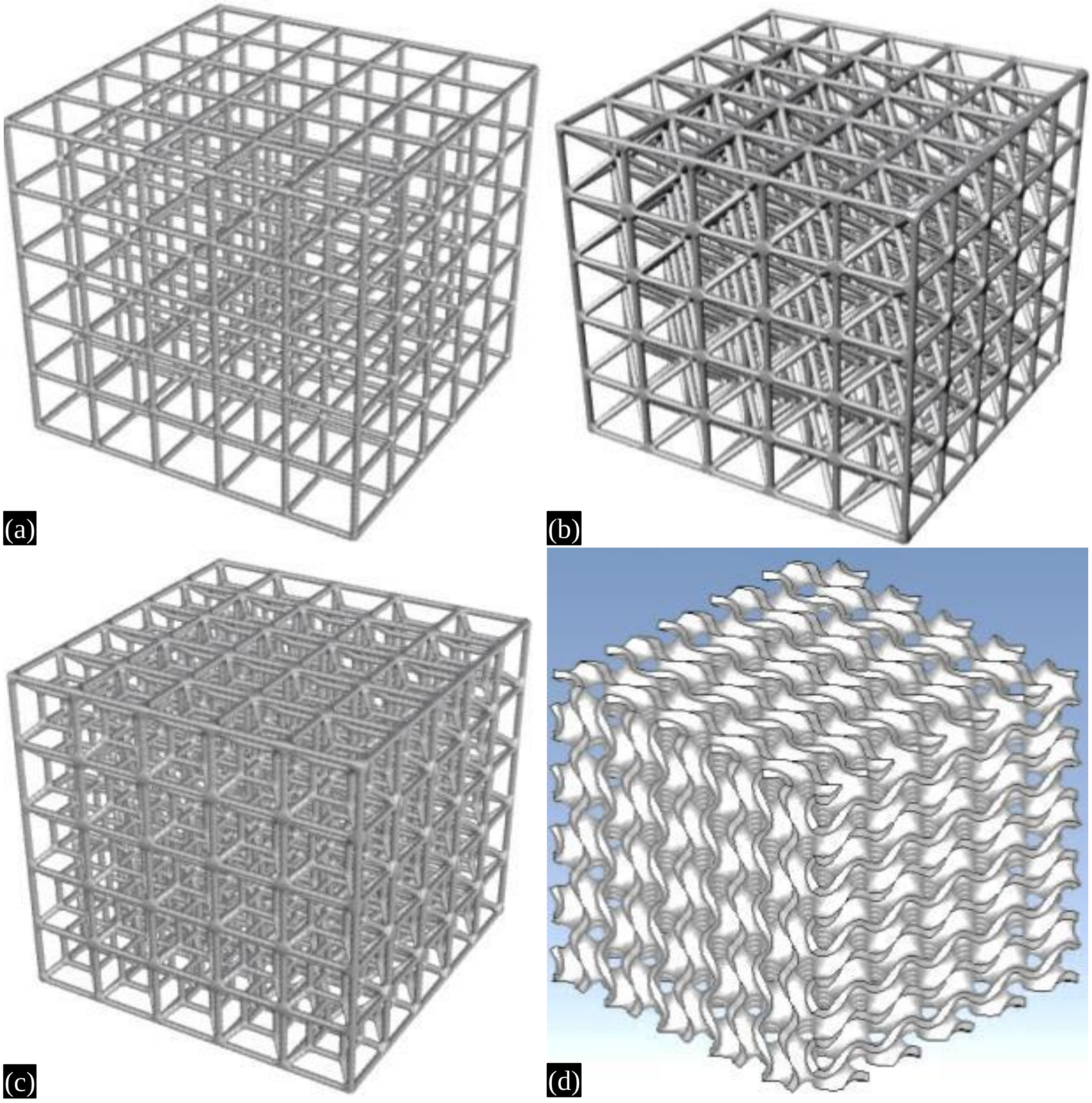

Figure 3. Unit cells comprised of 5×5×5 array. (a) Grid, (b) Star, (c) Tesseract, (d) Gyroid.

Table 1. Geometric properties of the four-unit cell (lattice) structure.

S.N.	N_{UC}	Unit cell size (SL)	Sd (mm)	PS (mm)	Number of units cell the pattern inX, Y, and Z-direction			Total lattice block dimensions approx.		
					Xn	*Yn*	*Zn*	*Length (mm)*	*Width (mm)*	*Height (mm)*
1.	Grid	2	0.5	1.5	5	5	5	10.52	10.52	10.52
2.	Star	2	0.5	1.5	5	5	5	10.52	10.52	10.52
3.	Tesseract	2	0.5	1.5	5	5	5	10.52	10.52	10.52
4.	Gyroid	2	0.5	-	5	5	5	10.16	10.16	10.16

Numerical Modeling Method

Using Altair Hyper Works, nonlinear finite element simulations were performed. The JC damage material model describes the elastoplastic behavior of nonlinear (implicit static) materials. To create finite element models for all CAD geometric structures, the input values of Young's modulus (E) (113.8 GPa) and Poisson ratio (0.34 GPa) of Ti6Al4V material, as well as the 3D mesh generated by tetrahedral

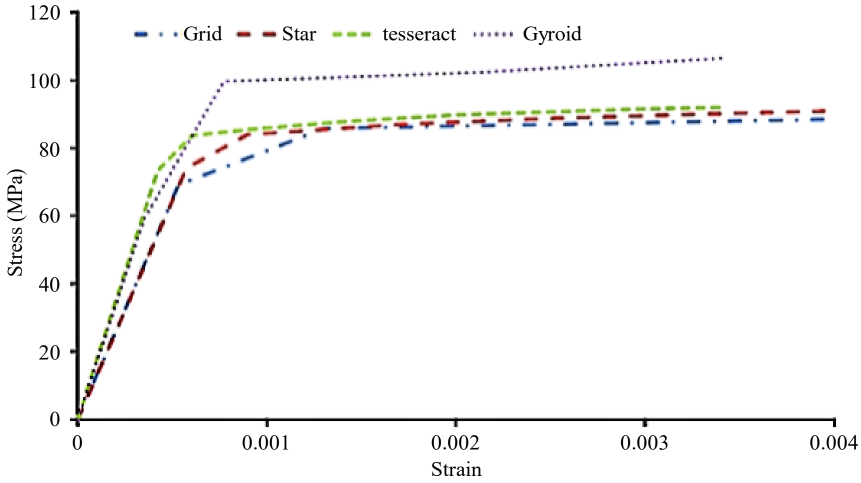

Figure 4. Stress-strain curve of grid, star, tesseract, and gyroid-based micro-lattice structures.

Table 2. Nonlinear finite element analysis for estimating mechanical responses with the Johnson-Cook material model.

S.N.	Unit cells or lattice-type	Compressive yield stress (YS)(MPa)	Estimate Young's modulus (E) (GPa)
1	Grid	69	1.01
2	Star	74	3.71
3	Tesseract	73	5.60
4	Gyroid	59	3.22

elements, were used. We examine the behavior of the stress-strain curve in biomaterials. Using the equation developed by Johnson-Cook (1983), characterize the flow stress of the material as the result of strain, strain rate, and temperature effects.

$$\sigma = \underbrace{[A + B\varepsilon_p^n]}_{\text{Strain hardening effect}} * \underbrace{\left[1 + C\,\text{In}\left(\frac{\varepsilon'}{\varepsilon'_0}\right)\right]}_{\text{Visco-plasticity behavior}} * \underbrace{[1 - T^{*m}]}_{\text{Thermal softening}}$$

Where, ε_p is the plastic strain, ε is the strain rate, and T is the temperature (in Kelvin). In this case, the visco-plasticity and thermal softening effects are neglected. Here, a is the yield strength, b is the hardening modulus, c is the strain rate sensitivity, and n is the hardening coefficient.

The star has a higher compressive yield (YS) stress than the other three lattice structures. The stress-strain graphs illustrate how the same uniaxial compressive load affects the mechanical properties of various unit cell shapes (Figure 4). Table 2 shows that the star lattice has the greatest yield stress under uniaxial compressive load when nonlinear finite element modeling is used.

Finite Element Model Validation Study

To determine the mechanical response of the Ti-6Al-4V lattice structure and to validate the FEA [24], evaluate the impact of strain rate in a quasi-static compression test. SLM, or selective laser melting, was used to create the f2cc-z structure. The 8×8×8 array makes up the f2cc-z lattice, which has struts that are 0.35 mm in diameter and cells that are 2 mm in width. According to experimental data, the compressive yield stress and Young's modulus are 1.5 GPa and 47 MPa, respectively. An identical model was developed, and the nonlinear simulation was performed as verification. According to the results of the finite element simulation, the values for Young's modulus and compressive yield stress are 2.51 GPa and 55 MPa, respectively. The FEA and 3D CAD model of the f2cc-z lattice structure are shown in Figure 5.

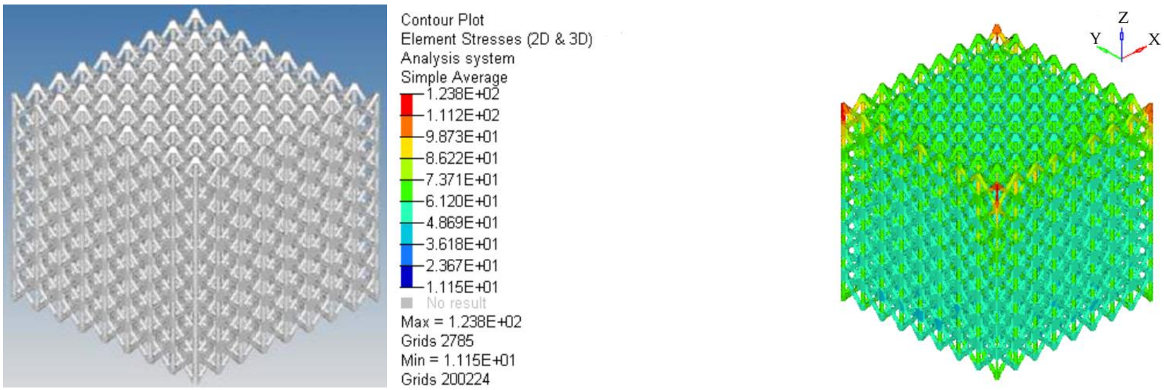

Figure 5. (a) 8×8×8 of f2cc-z unit cell 3D CAD model; (b) von Mises stress.

Optimize Design Parameters Using the Design of the Experiment

Demonstration that, among all other lattices, the star-based lattice has the highest yield stress. To build Ti-6Al-4V micro-lattice structures at three levels and two factors, namely strut diameter (Sd) and pore size (Ps), another star lattice is used. When combined, the design factors that have the most significant impact on the mechanical response for the same compressive loads are described in Tables 3 and 4. The L9 Taguchi orthogonal array was used to design of experiments (DOE). We created a nine-lattice structure model in the same 5×5×5 array for this early investigation using a new set of design parameters.

RESULTS AND DISCUSSION

The nine finite element simulation results show that the low-porosity micro-lattice scaffold structure possesses high compressive yield stress (YS) and low Young's modulus (E). The pore size and porosity of the porous scaffold structure should be appropriate to provide the requisite mechanical characteristics for the prosthetic application. Young's modulus of the micro-lattice scaffold structure must be low and closer to the modulus of human bone to decrease the stress-shielding effect. The similar compressive uniaxial loading condition resulted in high compressive yield stress (86 MPa), pore size (PS) (0.75 mm), and strut diameter (Sd) (0.25 mm) values, which were optimized using the DOE approach. Modification in the design factors of micro-lattice structures affects their mechanical characteristics. Micro-cellular porous biomaterial structures' pore size and porosity play a significant role in developing human bone tissues. Therefore, pore size and porosity must be suitable for all porous, cellular structures in biomedical

Table 3. Control factors and their levels.

Factor/Level	(Sd)	(Ps)
Level 1	0.25	0.75
Level 2	0.37	1.00
Level 3	0.50	1.25

Table 4. Taguchi L9 orthogonal array.

S.N.	(Sd)	(Ps)
1	0.25	0.75
2	0.25	1.00
3	0.25	1.25
4	0.37	0.75
5	0.37	1.00
6	0.37	1.25
7	0.50	0.75
8	0.50	1.00
9	0.50	1.25

Table 5. Geometric attribute of star micro-lattice structures.

S.N.	Unit cell	Number of the unit cell in the 3D array arrangement			Strutdiameter (Sd)	Poresize (PS)	Total block dimension in X, Y, and Z-axis			Vol. of the porous part	Volume of block	Porosity	Yield stress(YS)	Young's modulus (E)
		n x n x n			*(mm)*	*(mm)*	*(mm)*			*(mm^3)*	*(mm^3)*	*%*	*(MPa)*	*(GPa)*
1	Star	5	5	5	0.25	0.75	5.28	5.28	5.25	49.15	146.36	66.42	86	3.41
2		5	5	5	0.25	1	6.53	6.53	6.53	64.16	278.45	76.96	78	5.36
3		5	5	5	0.25	1.25	7.78	7.78	7.78	79.16	470.91	83.19	79	7.65
4		5	5	5	0.37	0.75	6.01	6.01	6.01	112.01	217.08	48.40	83	3.24
5		5	5	5	0.37	1	7.26	7.26	7.26	144.88	382.66	62.14	73	4.26
6		5	5	5	0.37	1.25	8.51	8.51	8.51	177.75	616.30	71.16	72	7.12
7		5	5	5	0.5	0.75	6.8	6.8	6.8	213.15	314.43	32.21	82	2.59
8		5	5	5	0.5	1	8.05	8.05	8.05	273.17	521.66	47.63	77	4.05
9		5	5	5	0.5	1.25	9.3	9.3	9.3	333.19	804.36	58.58	82	6.53

applications to provide the requisite mechanical properties. Using FEA, it was discovered that micro-lattice structures with high porosity had a high Young's modulus. Table 5 illustrates the relationship between porosity, compressive yield stress, and Young's modulus.

CONCLUSION

The FEA investigation revealed that the star has higher yield stress and lower Young's modulus (E) values than the grid, tesseract, and gyroid structures. Therefore, the Taguchi-based design of the experiment approach was offered to reduce the number of simulations run. Under the same compressive loads, the estimate of the mechanical characteristics of these structures was optimized for porosity, compressive yield stress, and Young's modulus. According to the results of the finite element simulation, it was also discovered that the porosity significantly impacts how mechanically responsive the Ti-6Al-4V micro-lattice scaffold structures are. The suggested research shows that Young's modulus value for the micro-lattice scaffold structure was between 2.59 and 7.65 GPa, comparable to the range of human cortical bone. Based on these results, we can say that the necessary mechanical properties can be obtained by changing the design parameters of the scaffold.

REFERENCES

1. Miao X, Graded SD. Gradient Porous Biomaterials. Materials (Basel). 2010;3(1):26–47. doi: 10.3390/ma3010026.
2. Wally Z, Van Grunsven W, Claeyssens F, Goodall R, Reilly G. Porous titanium for dental implant applications. Metals. 2015;5(4):1902–20. doi: 10.3390/met5041902.
3. Matassi F, Botti A, Sirleo L, Carulli C, Innocenti M. Porous metal for orthopedics implants. Clin Cases Miner Bone Metab. 2013;10(2):111–5.
4. Ryan GE, Pandit AS, Apatsidis DP. Porous titanium scaffolds fabricated using a rapid prototyping and powder metallurgy technique. Biomaterials. 2008;29(27):3625–35. doi: 10.1016/j.biomaterials.2008.05.032.
5. Ahsan MN, Paul CP, Kukreja LM, Pinkerton AJ. Porous structures fabrication by continuous and pulsed laser metal deposition for biomedical applications; modelling and experimental investigation. J Mater Process Technol. 2011;211(4):602–9. doi: 10.1016/j.jmatprotec.2010.11.014.

6. Vesenjak M, Ren Z. Yielding and post-yield behaviour of closed-cell cellular materials under multiaxial dynamic loading. Met Mater Int. 2016;22(3):435–42. doi: 10.1007/s12540–016–5550–7.
7. Buciumeanu M, Palaghian L, Miranda AS, Silva FS. Fatigue life predictions including the Bauschinger effect. Int J Fatigue. 2011;33(2):145–52. doi: 10.1016/j.ijfatigue.2010.07.012.
8. Zena JW, Grunsven WV, Claeyssens F, et al. Porous Titanium for Dental Implant Applications. In Metals. 2015; 5(4):1902-1920. https://doi.org/10.3390/met5041902.
9. Levine B. A new era in porous metals: applications in orthopaedics. Advanced Engineering Materials. Sep 2008; 10(9): 788-792..
10. Dabrowski B, Swieszkowski W, Godlinski D, Kurzydlowski KJ. Highly porous titanium scaffolds for orthopaedic applications. Journal of biomedical materials research Part B: Applied biomaterials. Oct 2010; 95(1): 53-61.
11. Yan C, Hao L, Hussein A, Raymont D. Evaluations of cellular lattice structures manufactured using selective laser melting. Int J Mach Tool Manuf. 2012;62:32–8. doi: 10.1016/j.ijmachtools.2012.06.002.
12. Ashby M, Evans A, Fleck N, Gibson L, Hutchinson J, Wadley H, et al. Metal foams: A design guide. Appl Mech Rev. 2001;54(6):B105–6. doi: 10.1115/1.1421119.
13. Nouri A, Hodgson PD, Wen C. Biomimetic porous titanium scaffolds for orthopedic and dental applications. Published online; 2010. p. 415–51.
14. Oladapo BI, Zahedi SA, Adeoye AOM. 3D printing of bone scaffolds with hybrid biomaterials. Compos B Eng. 2019;158:428–36. doi: 10.1016/j.compositesb.2018.09.065. https://doi:10.1016/j.compositesb.2018.09.065.
15. Oladapo BI, Zahedi SA, Ismail SO, Olawade DB. Recent advances in biopolymeric composite materials: future sustainability of bone-implant. Renew Sustain Energy Rev. 2021;150. doi: 10.1016/j.rser.2021.111505.
16. Oladapo BI, Ismail SO, Adebiyi AV, Omigbodun FT, Olawumi MA, Olawade DB. Nanostructural interface and strength of polymer composite scaffolds applied to intervertebral bone. Colloids Surf A Physicochem Eng Aspects. 2021;627. doi: 10.1016/j.colsurfa.2021.127190.
17. Oladapo BI, Zahedi SA, Omigbodun FT. A systematic review of polymer composite in biomedical engineering. Eur Polym J. 2021;154. doi: 10.1016/j.eurpolymj.2021.110534.
18. Oladapo BI, Zahedi SA, Ismail SO. Mechanical performances of hip implant design and fabrication with PEEK composite. Polymer. 2021;227. doi: 10.1016/j.polymer.2021.123865.
19. Oladapo BI, Zahedi SA. Improving bioactivity and strength of PEEK composite polymer for bone application. Mater Chem Phys. 2021;266. doi: 10.1016/j.matchemphys.2021.124485.
20. Oladapo BI, Zahedi SA, Ismail SO, Omigbodun FT. 3D printing of PEEK and its composite to increase biointerfaces as a biomedical material: A review. Colloids Surf B Biointerfaces. 2021;203:111726. doi: 10.1016/j.colsurfb.2021.111726.
21. Oladapo BI, Zahedi SA, Ismail SO, Omigbodun FT, Bowoto OK, Olawumi MA, et al. 3D printing of PEEK–cHAp scaffold for medical bone implant. Bio-Des Manuf. 2021;4(1):44–59. doi: 10.1007/s42242–020–00098–0.
22. Oladapo BI, Ismail SO, Bowoto OK, Omigbodun FT, Olawumi MA, Muhammad MA. Lattice design and 3D-printing of PEEK with Ca10(OH)(PO4)3 and in-vitro bio-composite for bone implant. Int J Biol Macromol. 2020;165(A):50–62. doi: 10.1016/j.ijbiomac.2020.09.175. https://doi:10.1016/j.ijbiomac.2020.09.175.
23. Oladapo BI, Obisesan OB, Oluwole B, Adebiyi VA, Usman H, Khan A. Mechanical characterization of a polymeric scaffold for bone implant. J Mater Sci. 2020;55(21):9057–69. doi: 10.1007/s10853–020–04638-y.
24. Merkt S, Hinke C, Bültmann J, Brandt M, Xie YM. Mechanical response of TiAl6V4 lattice structures manufactured by selective laser melting in quasistatic and dynamic compression tests. J Laser Appl. 2015;27(S1);Suppl 1:S17006. doi: 10.2351/1.4898835.

